Refinement of the Geophysical Fluid Dynamics Laboratory solar benchmark computations and an improved parameterization for climate models

S. M. Freidenreich and V. Ramaswamy
Geophysical Fluid Dynamics Laboratory, NOAA, Princeton, New Jersey, USA

Received 27 September 2004; revised 8 April 2005; accepted 26 May 2005; published 13 September 2005.

[1] A recent intercomparison study of solar radiative transfer models has revealed a notable difference (5%) in the total spectrum column absorptance, for a specified clear-sky atmospheric profile, between two principal line-by-line benchmark results (namely, the Geophysical Fluid Dynamics Laboratory (GFDL) and the Atmospheric and Environmental Research, Inc. models). We resolve this discrepancy by performing a series of "benchmark" computations which show that the water vapor continuum formulation, spectral line information, and spectral distribution of the solar irradiance at the top of the atmosphere are key factors. Accounting for these considerations reduces the difference between the two benchmarks to less than 1%. The analysis establishes a high level of confidence in the use of benchmark calculations for developing and testing solar radiation parameterizations in weather and climate models. The magnitude of the change in absorption in the newer GFDL benchmark computations, associated with the use of a more recent spectral line catalog and inclusion of the water vapor continuum, has also necessitated revising the solar parameterization used in the operational GFDL general circulation model (GCM). When compared with the newer reference computation, the older parameterization shows an underestimate of the clear-sky heating rate throughout the atmosphere, with the error in the atmospheric solar absorbed flux being about 20 W m^{-2} for a midlatitude summer atmosphere and overhead Sun. In contrast, the new parameterization improves the representation of the solar absorption and reduces the bias to about 5 W m^{-2}. Another important feature of the new parameterization is a nearly 50% reduction in the number of pseudomonochromatic columnar calculations compared to the older formulation, with only relatively small increases in the biases in absorption for cloudy layers. This yields a reduction of about 10% in the GCM computational time. The effect of the new parameterization on the simulated temperature in the new operational GFDL climate GCM is also examined. There is an increased solar heating; this yields temperature increases exceeding 1 K in the lower stratosphere.

Citation: Freidenreich, S. M., and V. Ramaswamy (2005), Refinement of the Geophysical Fluid Dynamics Laboratory solar benchmark computations and an improved parameterization for climate models, *J. Geophys. Res.*, *110*, D17105, doi:10.1029/2004JD005471.

1. Introduction

[2] Comparative studies of solar radiative transfer codes are useful in verifying the validity and accuracy of any given model. Having available high-resolution line-by-line (LBL) computations from more than one model adds a measure of confidence. Such a comparison of results, for a clear-sky atmosphere, was made possible by a recent study [*Barker et al.*, 2003] (hereinafter referred to as B03). Two LBL models were considered: GFDL [*Freidenreich and Ramaswamy*, 1999 (hereinafter referred to as FR99); *Ramaswamy and Freidenreich*, 1991] and Atmospheric Environmental Research, Inc. (AER), referred to elsewhere as "LBLRTM" [*Clough and Iacono*, 1995; *Clough et al.*, 1992]. Both LBL models are coupled to codes that use the doubling-adding (DA) technique [*Hunt and Grant*, 1969] for the treatment of multiple scattering, making them further comparable. For the AER model, this DA code has been referred to as "CHARTS" [*Moncet and Clough*, 1997], and the coupled LBL + DA code as "LBLRTM/CHARTS," and we adopt this nomenclature in the rest of this paper. Likewise, the GFDL model results are referred to as "LBL + DA" or simply as "GFDL."

[3] For the clear-sky case, a notable difference in the broadband absorptance was found to exist in the LBL + DA result relative to the LBLRTM/CHARTS result. Such differences are unacceptable in codes that are regarded as benchmarks to guide parameterizations in weather and climate models. One objective of this paper is to show

Table 1a. Comparison Between the LBL + DA and the LBLRTM/CHARTS Models for TOA Albedo (α_p), Atmospheric Absorptance (a_{atm}) and Surface Absorptance (a_{sfc}) for the Prescribed Clear-Sky Case by B03[a]

				0.2–5.0 μm			0.2–0.7 μm			0.7–5.0 μm		
Model	HITRAN Catalog	H_2O Continuum	S TOA	α_p	a_{atm}	a_{sfc}	α_p	a_{atm}	a_{sfc}	α_p	a_{atm}	a_{sfc}
LBL + DA	1992	none	LN	0.191	0.230	0.579	0.266	0.085	0.649	0.126	0.356	0.518
LBL + DA	2000	none	LN	0.191	0.232	0.577	0.266	0.085	0.649	0.125	0.362	0.513
LBL + DA	2000	CKD2.1	LN	0.189	0.240	0.571	0.266	0.085	0.649	0.122	0.376	0.502
LBL + DA	2000	CKD2.1	K	0.188	0.242	0.570	0.260	0.093	0.647	0.122	0.376	0.502
LBLRTM/CHARTS	1996	CKD2.1	K	0.190	0.243	0.567	0.267	0.091	0.642	0.121	0.380	0.499

[a]Results are presented for the total solar ($0.2 < \lambda < 5.0$ μm) and for the ultraviolet + visible ($0.2 < \lambda < 0.7$ μm) and near-infrared ($0.7 < \lambda < 5.0$ μm) regions separately. The cosine of the solar zenith angle (μ_0) is set to 0.5. The LBL + DA results submitted to that study were based on the 1992 HITRAN catalog, without the inclusion of the H_2O continuum, and the *Labs and Neckel* [1970] (LN) solar irradiance (S) values at the top of atmosphere (TOA). The LBLRTM/CHARTS model used the 1996 HITRAN catalog, with the inclusion of the CKD 2.1 H_2O continuum, and solar irradiance values taken from *Kurucz* [1994] (K). Results are also presented when the 2000 HITRAN database is used, the CKD2.1 continuum is included, and the K solar irradiance values are applied, in the LBL + DA model computations.

that, upon systematic considerations of different factors in the context of the GFDL model, the differences are reduced and the two benchmark models are shown to be in excellent agreement.

[4] The updating of the LBL + DA model calculations due to incorporating some of these factors, as explained below, has also necessitated a revision of the solar parameterization used previously in the operational GFDL GCM (FR99). In doing so, we have also taken into consideration the need to update the code to reduce the computational time involved. We also examine how the updated code affects the accuracy of the new parameterization in the case of overcast atmospheres. Finally, the effect of the new parameterization on the temperature response in the new GFDL climate GCM [*Anderson et al.*, 2004] is examined.

2. Results

2.1. Benchmark Computations

[5] The GFDL LBL model has a very high fixed vertical (122 layers) and spectral (<0.005 cm^{-1}, on average) resolution for treating the absorptive properties of the various gases considered in this study (CO_2, H_2O and O_2). We focus on P > 10 mbar, since changes in the heating rate due to the factors considered in this study become negligible above it. Further details and references regarding the development of the model and its usage have been described [e.g., *Ramaswamy and Freidenreich*, 1991; FR99]

[6] The LBL + DA and LBLRTM/CHARTS model results for the prescribed clear-sky atmosphere discussed by B03 are shown in Table 1a. These are presented in terms of broadband averages of the top of atmosphere (TOA) albedo, atmospheric and surface absorptance for the total solar ($0.2 < \lambda < 5.0$ μm), ultraviolet + visible ($0.2 < \lambda < 0.7$ μm), and near-infrared ($0.7 < \lambda < 5.0$ μm) spectra, respectively. The spectra are defined in Table 5a of B03. The GFDL results reported by B03 used the 1992 HITRAN [*Rothman et al.*, 1992] database without the H_2O continuum, while the LBLRTM/CHARTS model used the 1996 HITRAN [*Rothman et al.*, 1998] database with CKD version 2.1 for the H_2O continuum [*Clough et al.*, 1992]. Most notably, the LBL + DA total spectral atmospheric absorptance underestimates the LBLRTM/CHARTS value by 5%, with a corresponding overestimate in the surface absorptance. The TOA reflectance agrees quite well between the two models.

[7] A series of experiments is performed to investigate the effect of bringing more into agreement the assumptions considered in the two models. In particular, we inquire into the issue of reducing the difference in the results between the two models. In the first experiment (see Table 1a), the LBL + DA model uses a more up-to-date prescription of the absorption coefficients, derived from the HITRAN 2000 line catalog [*Rothman et al.*, 2003]. The resulting increase in solar absorption reduces the original difference in the atmospheric and surface absorptance between the two models e.g., by ~25% in the near infrared. Computations with the individual gases show that the updated line parameters for H_2O contribute mostly toward the increase in absorption. We next investigate the effect of inclusion of the H_2O continuum on further reducing the difference between the two models. Note that the influence of the continuum has also been investigated elsewhere [*Iacono et al.*, 2000; *Tarasova and Fomin*, 2000]. When the CKD 2.1 H_2O continuum is incorporated, an additional reduction of even larger magnitude (>50%) occurs in the original difference for the near infrared, so that the resulting broadband quantities for the near-infrared and total spectrum now agree to about 1% between the two models.

[8] With these updates, however, there still remains a notable difference (7%) for the atmospheric absorptance value in the ultraviolet + visible spectral region. After further analysis of the assumptions used in the LBLRTM/CHARTS model (Mlawer, personal communication, 2003), significant differences are found to exist between the two

Table 1b. Comparison of the Integrated Solar Flux Values at the TOA for Various Spectral Regions, Between the LN and K Data Sets for $\mu_0 = 0.5$

		TOA Solar flux, W m^{-2}			
Model	S TOA	0.7–5.0 μm	0.4–0.7 μm	0.2–0.4 μm	0.2–5.0 μm
LBL + DA	LN	360.5	263.6	51.8	675.9
LBLRTM/CHARTS	K	358.1	266.4	56.7	681.2

Table 1c. Comparison of the Changes in the Three Quantities Presented in Table 1a in the LBL + DA Model due to Use of the K Data for the Ultraviolet ($0.2 < \lambda < 0.4$ μm) and Visible ($0.4 < \lambda < 0.7$ μm) Regions Separately

				0.2–0.4 μm			0.4–0.7 μm		
Model	HITRAN Catalog	H_2O Continuum	S TOA	α_p	a_{atm}	a_{sfc}	α_p	a_{atm}	a_{sfc}
LBL + DA	2000	CKD2.1	LN	0.330	0.251	0.419	0.254	0.052	0.694
LBL + DA	2000	CKD2.1	K	0.302	0.284	0.414	0.251	0.053	0.696

models in the specification of the TOA solar irradiance. The LBL + DA model uses the *Labs and Neckel* [1970] data, with a spectral resolution of hundreds or even thousands of wave numbers, while the LBLRTM/CHARTS model uses data taken from *Kurucz* [1994], which has a one wave number resolution throughout the spectrum. Also, the magnitude of the integrated solar flux differs significantly between the two models.

[9] Table 1b presents the solar flux values at the TOA in these two data sets, for the zenith angle considered and for the spectral ranges defined by B03. Most of the difference occurs in the ultraviolet + visible region, particularly in the ultraviolet. We next investigate how the convolution of the spectral dependences of the solar irradiance and the gas absorption affect the value of the broadband absorptance. For this, we use the LBLRTM/CHARTS solar irradiance values in the LBL + DA model. This increases the atmospheric absorptance in the ultraviolet + visible region, so that the LBL + DA value is now greater than the LBLRTM/CHARTS value, but with a smaller absolute difference than before. In Table 1c, the resulting quantities for the visible and ultraviolet are determined separately to compare the effect of changing the solar data in the LBL + DA model. Note that nearly all the contribution toward this increase in atmospheric absorptance occurs in the ultraviolet. This may be explained by the fact that the Labs and Neckel data has its coarsest resolution in the ultraviolet (>1000 cm^{-1}); this is in contrast to the very high resolution in LBLRTM/CHARTS. For the total spectrum, there is a further reduction in the differences (<1%) for the atmospheric and surface absorptance values between the two models.

[10] There still are some issues that could impact the remaining differences seen. The values and spectral resolution of the O_3 cross sections are different between the two models. This could affect the ultraviolet + visible absorptance calculation in the LBL + DA model, particularly if it is convolved with the high-resolution specification of the solar irradiance used in the LBLRTM/CHARTS model. Additionally, differences in the LBL-determined absorption coefficients between the two models, due either to possible changes between the 2000 and 1996 HITRAN line catalogs, or to the exact way the frequency spectrum is partitioned, may explain some of the remaining differences seen in the near infrared. We also note here that more significant differences exist in the values obtained between the two models for the plane-parallel cloud cases considered by B03. This is likely due to differences in the prescription of drop optical properties: the LBL + DA model used the *Slingo* [1989] formulation, while the LBLRTM/CHARTS model values were based on a Mie calculation. These issues, however, are beyond the scope of this study.

[11] Overall, we have verified that the original differences seen between the two models are primarily due to: exclusion of the H_2O continuum; use of an older HITRAN line catalog; and coarser spectral specifications of the solar irradiance at the top of the atmosphere. We retain the prescription derived by *Labs and Neckel* [1970] of solar irradiance for the LBL + DA model calculations in the rest of this study.

[12] The change in the clear-sky solar heating due to use of HITRAN 2000 and inclusion of the CKD 2.1 H_2O continuum is illustrated in Figure 1, considering a midlatitude summer (MLS) climatological profile [*McClatchey et al.*, 1972]. The results for two zenith angles are shown, 0° and 75°. There is an increased heating (mostly > 5%) in the troposphere, due mainly to inclusion of the continuum. The corresponding change in the absorbed flux in the atmosphere is likewise notable, e.g., from 233.7 W m^{-2} to 244.9 W m^{-2} for the overhead Sun case. The spectral distribution of the change in the cumulative heating rate, i.e., the heating rate summed with increasing wave number, associated with the updated benchmark result, is illustrated in Figure 2 for the overhead Sun case. Virtually all the contribution toward increased heating occurs in the near infrared. Of interest is the strong dependence on height of the spectral region where the differences flatten out with increasing wave number. This varies from about 7000 cm^{-1} near the tropopause to about 17,000 cm^{-1} near the surface, and is indicative of the general trend of

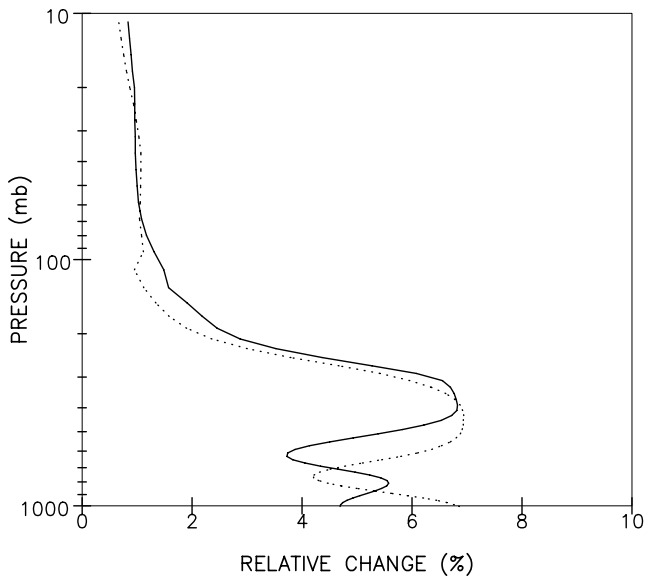

Figure 1. Relative change (percent) in the clear-sky solar heating rate between that due to the 2000 HITRAN database with the CKD 2.1 water vapor continuum included and that due to the 1992 database without the continuum. A midlatitude summer (MLS) atmosphere is considered, and the CO_2 amount is 346 ppmv. Results are shown for two solar zenith angles: 0° (solid line) and 75° (dotted line).

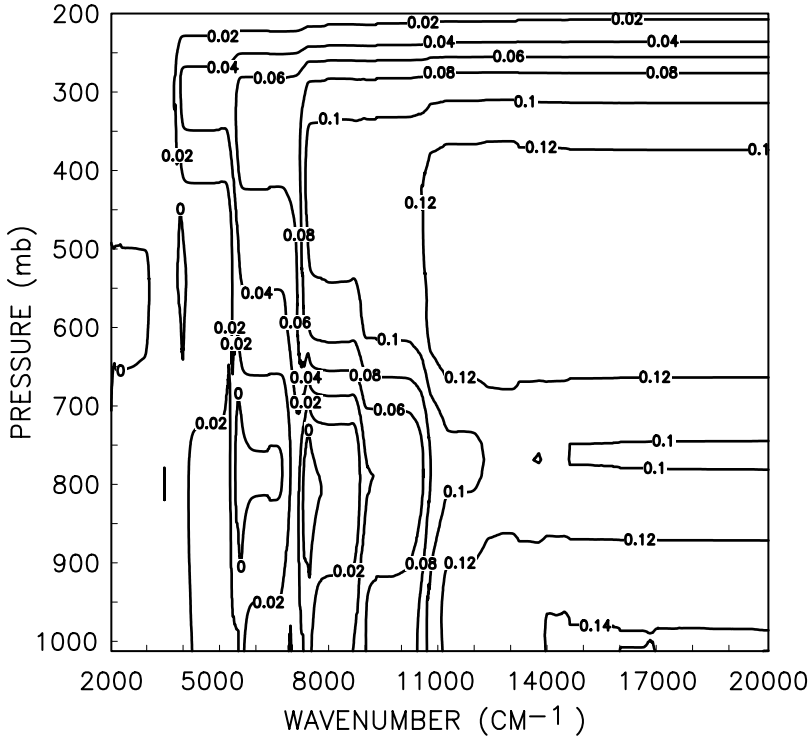

Figure 2. Cumulative change (K d^{-1}) in the clear-sky solar heating rate due to the 2000 (with CKD 2.1) HITRAN database. A MLS atmosphere and overhead Sun are considered.

weakening H_2O absorption in the column with increasing wave number.

2.2. Parameterization

[13] The magnitude of the increased absorption associated with these updates in the benchmark results necessitates a revision of the parameterization presented by FR99. First, however, another issue needs to be addressed in connection with that parameterization. Although it has been used in a number of studies involving the GFDL SKYHI GCM [*Ramachandran et al.*, 2000; *Haywood et al.*, 1999], the number of pseudomonochromatic columnar calculations required make it computationally prohibitive for use in the new GFDL climate model [*Anderson et al.*, 2004]. This is due in part to a reduction in the radiative time step in the new model, which significantly increases the relative amount of computational time expended for the shortwave radiation calculations. In response, and as part of revising the solar parameterization, we also seek to reduce the number of pseudomonochromatic columnar calculations needed, and thus reduce the computational burden in the GCM.

[14] In developing the FR99 parameterization, most of the computational burden that arose resulted from the need to minimize the error in the cloud absorbed flux relative to benchmark calculations. The basis for this determination was the use of the prescribed optical properties from the ICRCCM [*Ellingson and Fouquart*, 1991] "CS" (small drops) and "CL" (large drops) size distributions. FR99 showed that significant improvements in accuracy occurred in the 2500–4200 cm^{-1} and 4200–8200 cm^{-1} spectral regions when the bands were further partitioned. However, this also increased the number of pseudomonochromatic columnar calculations, because of more exponential-sum-fit [*Wiscombe and Evans*, 1977] terms required to model H_2O absorption over the narrower band regions. The new GCM uses a prescription of drop optical properties that are derived from the *Slingo* [1989] formulation, specified over wider spectral widths. There is now less of a degradation in the accuracy of the cloud absorbed flux because of leaving these two spectral regions as single bands, as will be illustrated later. Thus the number of concerned bands is now reduced from 7 to 2, and the number of required pseudomonochromatic columnar calculations reduced from 36 to 17 for the 2500–8200 cm^{-1} region.

[15] Three other simplifications are made to reduce the computational expense involved. First, the absorption by H_2O in the 0–2500 cm^{-1} region is ignored. Although about one half to two thirds of the incoming solar irradiance in this band is absorbed by H_2O in a clear-sky atmosphere, depending on the solar zenith angle, this represents only 2–3% of the total spectral absorption. However, this assumption will yield greater inaccuracies in the heating profile in that band. This simplification reduces the number of pseudomonochromatic columnar calculations in that band from 6 to 1. Second, the number of pseudomonochromatic columnar calculations in the 8200–14600 cm^{-1} region is reduced from 15 to 7. Third, the number of bands in the 27,500–34,500 cm^{-1} region is reduced from 5 to 3. Overall, these three simplifications do not impact the maximum errors observed in the total solar heating. Thus there is a reduction in the number of bands from 25 to 18, and in the number of pseudomonochromatic intervals from 72 to 38. The same numerical techniques and "best fit" criteria described by FR99 are followed here to fit the new heating rate profiles for the individual

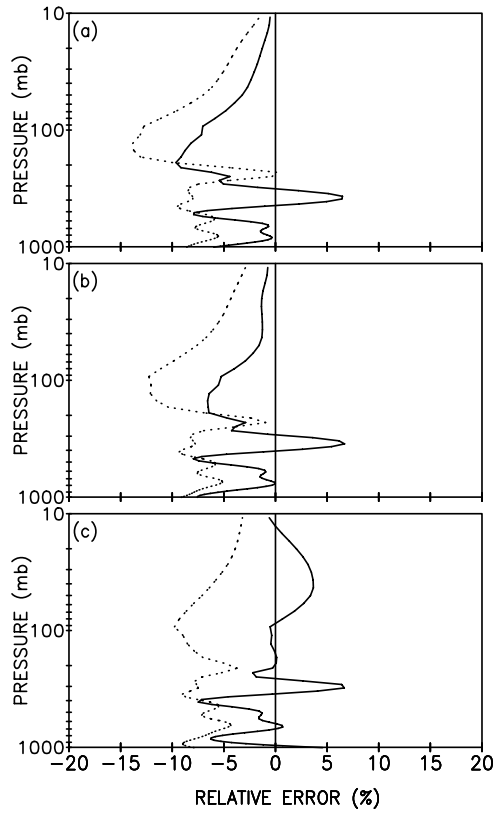

Figure 3. Relative error in the clear-sky solar heating rate, with respect to the reference derived from the HITRAN 2000 database (with CKD 2.1) for the FR99 solar parameterization (dotted line) and the new parameterization (solid line). A MLS atmosphere is assumed, and the solar zenith angle is set to (a) 0°, (b) 53°, and (c) 75°.

gases. (The coefficients for these fits are available from the authors upon request.) Note that, in the context of the current operational GFDL climate GCM, these simplifications reduce the computational time taken by 10%.

[16] Figures 3 and 4 show the error in the clear-sky heating rate derived from the FR99 shortwave parameterization and the new parameterization. Both are with respect to reference cases which are based on the HITRAN 2000 database (CKD 2.1 continuum included). We consider three climatological profiles [*McClatchey et al.*, 1972]: MLS, tropical and subarctic winter (SAW), and three solar zenith angles: 0°, 53° and 75° (not all combinations are shown). Figure 3 shows the results for the MLS profile and the three solar zenith angles, while Figure 4 shows the corresponding results for the remaining profiles. There is an underestimate of heating throughout the troposphere and lower stratosphere in the old parameterization, which the new one partially corrects. For the 75° cases, there can be a slight overestimate of the heating in the lower stratosphere. The maximum error is generally <10%, but slightly higher for the tropical atmosphere. For the overhead Sun and MLS atmosphere case, the resulting error in the absorbed flux in the atmosphere is about 20 W m^{-2} (8%) and 5 W m^{-2} (2%), for the old and new parameterizations, respectively. Thus, despite the nearly 50% reduction in the number of pseudomonochromatic columnar calculations, the maximum relative error in the total clear-sky heating is kept to a small bias.

[17] The accuracy of the new formulation for overcast atmospheres, specifically the absorbed flux in the cloud, is examined in Table 2 for a small sample of cloud configurations. The corresponding errors based on the FR99 parameterization and older reference results are included for comparison. Also presented are the reference LBL + DA values. It is noteworthy that the magnitude of the relative error in the cloud absorbed flux has slightly increased in the high optically thin Slingo clouds (cases 1, 2 and 4). This is because of the coarsening of spectral intervals in the 2500–8200 cm^{-1} region compared to the older formulation. This tends to underestimate the cloud absorption in this region when both drops and H_2O are significantly contributing (FR99). The absolute changes (1–2 W m^{-2}) are, however, small for climate bias considerations, and would not be expected to impact the climate response in any significant manner. This effect of this coarsening, however, is more notable for case 5. Here a high, optically thin cloud is considered using the CS drop optical properties, for both the LBL + DA reference and parameterization calculations. Although the underestimate in the parameterized cloud absorbed flux can be ~10% for a similar Slingo-type cloud, it exceeds 20% for the CS-type cloud. Thus, while the two-band framework in the 2500–8200 cm^{-1} region is acceptable in conjunction with the use of Slingo-type clouds in the GCM, caution needs to be exercised in instances where a

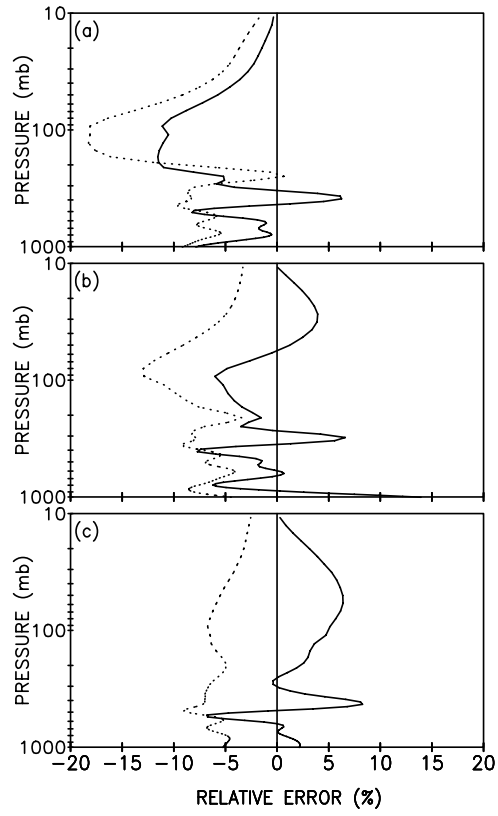

Figure 4. As in Figure 3 assuming the following combination of atmosphere and solar zenith angle: (a) tropical and 0°, (b) tropical and 75°, and (c) subarctic winter and 75°.

Table 2. Relative Error for the Cloud Absorbed Solar Flux, Comparing the FR99 and New Parameterization With the Reference Results Derived From the 1992 HITRAN (Without the H_2O Continuum) and 2000 HITRAN (With CKD 2.1 Continuum) Databases, Respectively[a]

		Solar Zenith Angle = 0°				Solar Zenith Angle = 75°			
		1992		2000		1992		2000	
Case	Cloud	Percent	Watts per Square Meter	Percent	Watts per Square Meter	Percent	Watts per Square Meter	Percent	Watts per Square Meter
1		<1	19.6	−10	19.7	−5	10.2	−11	10.2
2		−3	24.5	−10	24.2	−6	10.8	−11	10.8
3		−3	245.1	−1	247.1	3	38.7	2	38.9
4	1	−3	19.0	−10	19.1	−6	8.5	−11	8.6
	2	−4	86.2	−6	85.9	5	11.0	4	11.0
	3	2	40.0	5	39.3	10	5.0	12	5.0
5		4	16.4	−29	16.5	4	7.6	−21	7.6

[a]A midlatitude summer (MLS) [*McClatchey et al.*, 1972] profile and a CO_2 amount of 346 ppmv are assumed. The specification of drop optical properties is based on either the Slingo 24-band formulation (cases 1–4) or the ICRCCM CS size distribution (case 5). Results are shown for two solar zenith angles, 0° and 75°, and for the spectral region $\nu > 2500\ cm^{-1}$. Also shown in parentheses are the LBL + DA reference values. The cloud cases are as follows: (1) 180–200 mbar, optical depth is 1, effective radius is 10 μm, surface albedo is 0; (2) same as case 1 except surface albedo is 0.8; (3) 300–800 mbar, optical depth is 100, effective radius is 15 μm, surface albedo is 0; (4) 180–200 mbar, 480–500 mbar, and 880–900 mbar, optical depth is 1, 10, and 50, respectively, effective radius is 5, 10, and 10 μm, respectively, surface albedo is 0; and (5) 180–200 mbar, optical depth is 1, surface albedo is 0. For case 4, clouds 1, 2, and 3 correspond to the high, middle, and low cloud, respectively.

higher spectral resolution specification of drop optical properties is applied. Otherwise, for low, middle and geometrically thick clouds, the errors in the cloud absorbed flux are similar to that due to the older parameterization.

2.3. GCM Results

[18] We next examine the effect of the new parameterization on the simulated temperature in the new GFDL climate GCM. The model contains 24 levels in the vertical, with 4 of them in the stratosphere (P < 100 mbar). The model is integrated for 17 years, using the observationally based Atmospheric Model Intercomparison Project II SST and sea ice prescriptions, starting from January 1982 [*Anderson et al.*, 2004]. Two runs are performed: one using the FR99 parameterization and another using the new parameterization.

[19] Figure 5a shows the relative change (i.e., (new-old)/old) in the zonally, annually averaged clear-sky solar heating rate. There is an increase in the atmospheric heating, indicative of the increased absorption due to consideration of the HITRAN 2000 line catalog and inclusion of the H_2O continuum (see reference result in Figure 1). The largest changes occur in the middle troposphere and lower stratosphere. In the lower stratosphere the relative difference between the new and old parameterized heating is consistently larger than that between the new and old reference heating, seen in Figure 1. We perform two tests to confirm that the stratospheric difference seen in Figure 5a is principally due to the biases in the parameterizations. First, the instantaneous heating difference between the new and old parameterization is analyzed with the same climatological H_2O profiles. The relative increase for the lower stratosphere then is close to that observed in Figure 5a. For instance at 100 mbar, this difference ranges from 7–12%, with the largest values occurring for the 75° zenith angle and SAW conditions, consistent with the maximum difference seen in the polar regions in Figure 5a. Secondly, the influence of the difference in stratospheric moisture between the two GCM integrations is analyzed to determine its relative importance on the difference seen in Figure 5a. Overall, there is more zonally, annually averaged column H_2O mixing ratio in the new GCM run, with a maximum change of 4×10^{-7} kg kg^{-1} (10%) at 100 mbar. Using the new parameterization and adding this additional amount of moisture contributes to a <1% increase in the instantaneous heating. Thus differences in moisture that arise between the two GCM integrations are only a minor factor in the difference in heating seen for the lower stratosphere in Figure 5a.

[20] Figure 5b shows the resulting change in the simulated temperature, with the region of statistical significance at the 95% level also highlighted. The temperature increases in the troposphere, generally by a few tenths of a degree, with the results for middle latitudes deemed significant. Larger and more statistically significant changes exceeding 1 K occur in the lower stratosphere, because of the sensitivity of that region to heating perturbations. These lower stratospheric temperature changes are larger than what would be expected due solely to the (new-old) reference heating, as a result of the aforementioned parameterization heating biases. Compared with temperature observations from a 50-year climatology derived from the National Center for Environmental prediction (NCEP) reanalysis [*Kalnay et al.*, 1996], the control run containing the older parameterization exhibits a warm stratosphere and cold troposphere bias, with maximum differences of 4 K and 2 K, respectively. Thus the changes due to the new parameterization aid in slightly reducing this bias in the troposphere, but increasing it slightly in the stratosphere, which is likely related to the coarse vertical resolution of the model in the upper layers. Note that there could also be uncertainties in the NCEP stratospheric temperatures owing in part to observational uncertainties.

3. Conclusions

[21] The need to conduct an analysis of the effects due to various factors on the benchmark computation of solar absorption, plus the need to revise a shortwave parameterization based on this knowledge, has been largely motivated by the results of the B03 solar radiative transfer intercom-

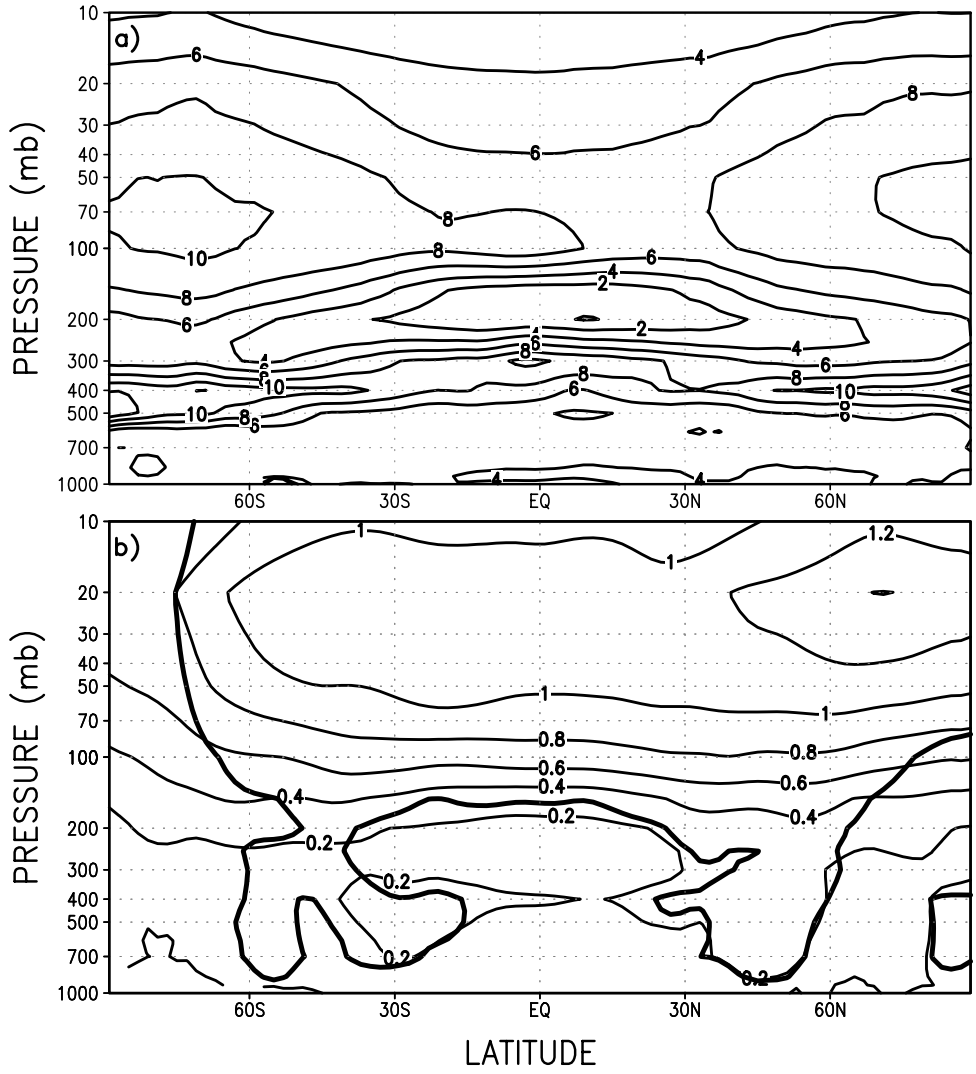

Figure 5. (a) The relative change (%) in the solar heating rate and (b) the change (K) in the temperature in the Geophysical Fluid Dynamics Laboratory general circulation model between the new and old solar radiation parameterization. Results are presented as zonal annual averages, based on a 17-year integration, using Atmospheric Model Intercomparison Project II prescribed sea surface temperatures and sea ice. Also shown in Figure 5b (thicker contour) is the region of statistical significance at the 95% level.

parison study. The inclusion of the H_2O continuum and updates of the H_2O line parameters in the LBL + DA model enhance the solar absorption. We have demonstrated here that there is now very good agreement (<1%) in the clear-sky absorbed solar flux in the atmosphere, between the LBL + DA and the LBLRTM/CHARTS models. Also, the fact that both models utilize the doubling-adding technique was useful in this assessment. The agreement between the two models occurs despite the fact that they have been developed independently and have a differing historical evolution. Demonstrating the agreement has proved to be a key benefit for the LBL + DA model and enables a higher level of confidence to be placed in it.

[22] The new parameterization presented here has also taken into account the need to reduce the computational time associated with using it. The simplifications result in a reduction of about 10% in the GCM computational time taken. For clear skies, the errors in heating are comparable to what was seen previously by FR99 with respect to older reference computations. However, for overcast skies, the reduction in the number of bands in the near infrared has somewhat increased the relative errors in the cloud absorbed flux for Slingo-type clouds, but the absolute errors remain small; however, the errors increase significantly (up to 30%) for CS-type optically thin high clouds. In response to the increased solar heating, there is a nominal increase in the atmospheric temperature in the new GFDL GCM, especially in the lower stratosphere. These changes aid in reducing a cold bias present in the troposphere.

[23] For future considerations, there remains the need to examine how well the LBL + DA and LBLRTM/CHARTS models agree in overcast sky situations when the exact same specifications of drop optical properties are used. On the basis of the changes seen in the LBL results because of how the solar irradiance at the top of the atmosphere is specified, there is also a need to examine the effect of a more updated

prescription of solar irradiance on the GCM's climate response.

References

Anderson, J. L., et al. (2004), The new GFDL global atmosphere and land model AM2–LM2: Evaluation with prescribed SST simulations, *J. Clim.*, *17*, 4641–4673.

Barker, H. W., et al. (2003), Assessing 1D atmospheric solar radiative transfer models: Interpretation and handling of unresolved clouds, *J. Clim.*, *16*, 2676–2699.

Clough, S. A., and M. J. Iacono (1995), Line-by-line calculations of atmospheric fluxes and cooling rates. 2: Application to carbon dioxide, ozone, methane, nitrous oxide, and the halocarbons, *J. Geophys. Res.*, *100*, 16,519–16,535.

Clough, S. A., M. J. Iacono, and J.-L. Moncet (1992), Line-by-line calculations of atmospheric fluxes and cooling rates: Application to water vapor, *J. Geophys. Res.*, *97*, 15,761–15,785.

Ellingson, R. G., and Y. Fouquart (1991), The intercomparison of radiation codes in climate models (ICRCCM): An overview, *J. Geophys. Res.*, *96*, 8926–8929.

Freidenreich, S. M., and V. Ramaswamy (1999), A new multiple-band solar radiative parameterization for general circulation models, *J. Geophys. Res.*, *104*, 31,389–31,409.

Haywood, J. M., V. Ramaswamy, and B. J. Soden (1999), Tropospheric aerosol climate forcing in clear-sky satellite observations over the oceans, *Science*, *283*, 1299–1303.

Hunt, G. E., and I. P. Grant (1969), Discrete space theory of radiative transfer and its application to problems in planetary atmospheres, *J. Atmos. Sci.*, *26*, 963–972.

Iacono, M. J., E. J. Mlawer, S. A. Clough, and J.-J. Morcrette (2000), Impact of an improved longwave radiation model, RRTM, on the energy budget and thermodynamic properties of the NCAR community climate model, CCM3, *J. Geophys. Res.*, *105*, 14,873–14,890.

Kalnay, E., et al. (1996), The NCEP/NCAR 40-year reanalysis project, *Bull. Am. Meteorol. Soc.*, *77*, 437–471.

Kurucz, T. L. (1994), *Infrared Solar Physics: Proceedings of the 154th Symposium of the International Astronomical Union, Held in Tucson, Arizona, U.S.A., March 2–6*, 1992, edited by D. M. Rabin, J. T. Jefferies, and C. Lindsey, 608 pp., Springer, New York.

Labs, D., and H. Neckel (1970), Transformation of the absolute solar radiation data into the international temperature scale of 1968, *Sol. Phys.*, *15*, 79–87.

McClatchey, R. A., R. W. Fenn, J. E. A. Selby, F. E. Volz, and J. S. Garing (1972), Optical properties of the atmosphere, *Rep. AFCRL-72–0497*, 110 pp., Hanscom Air Force Base, Bedford, Mass.

Moncet, J. L., and S. A. Clough (1997), Accelerated monochromatic radiative transfer for scattering atmospheres: Application of a new model to spectral radiance observations, *J. Geophys. Res.*, *102*, 21,853–21,866.

Ramachandran, S., V. Ramaswamy, G. L. Stenchikov, and A. Robock (2000), Radiative impact of the Mount Pinatubo volcanic eruption: Lower stratospheric response, *J. Geophys. Res.*, *105*, 24,409–24,429.

Ramaswamy, V., and S. M. Freidenreich (1991), Solar radiative line-by-line determination of water vapor absorption and water cloud extinction in inhomogeneous atmospheres, *J. Geophys. Res.*, *96*, 9133–9157.

Rothman, L. S., et al. (1992), The HITRAN molecular database: Editions of 1991 and 1992, *J. Quant. Spectrosc. Radiat. Transfer*, *48*, 469–507.

Rothman, L. S., et al. (1998), The HITRAN molecular spectroscopic database and HAWKS (HITRAN Atmospheric Workstation): 1996 edition, *J. Quant. Spectrosc. Radiat. Transfer*, *60*, 665–710.

Rothman, L. S., et al. (2003), The HITRAN molecular spectroscopic database: Edition 2000 including updates through 2001, *J. Quant. Spectrosc. Radiat. Transfer*, *82*, 5–44.

Slingo, A. (1989), A GCM parameterization of the shortwave radiative properties of water clouds, *J. Atmos. Sci.*, *46*, 1419–1427.

Tarasova, T. A., and B. A. Fomin (2000), Solar radiation absorption due to water vapor: Advanced broadband parameterizations, *J. Appl. Meteorol.*, *39*, 1947–1951.

Wiscombe, W. J., and J. W. Evans (1977), Exponential-sum fitting of radiative transmission functions, *J. Comput. Phys.*, *24*, 416–444.

S. M. Freidenreich and V. Ramaswamy, Geophysical Fluid Dynamics Laboratory, NOAA, P.O. Box 308, Princeton, NJ 08542, USA. (stuart.freidenreich@noaa.gov)